ChemPubSoc Europe

DOI: 10.1002/cphc.201900803

CHEMPHYSCHEM Articles

Tuning the Properties of Tetracene-Based Nanoribbons by Fluorination and N-Doping

Umer Younis,[a] Imran Muhammad,[a] Yoshiyuki Kawazoe,[b, c] and Qiang Sun*[a, d]

The structural stabilities and electronic properties are studied for the recently synthesized one-dimensional (1-D) tetracene-based nanoribbons with four-membered rings by using first-principles calculation. All three configurations (named as straight, zigzag, and armchair) are stable and exhibit an indirect band gap of 1.46, 0.73, and 0.32 eV, respectively. The band gaps can be effectively tuned by substituting hydrogen with fluorine atoms and by doping with nitrogen atoms. Substituting hydrogen with fluorine atoms leads to gradual decrease of the electronic band gaps of all configurations. Nitrogen doping changes the band gap from indirect to direct, displaying flexibility of tuning the band structure.

1. Introduction

Carbon-based materials, including graphene,[1] acene-based nanoribbons (NRBs),[2–4] fullerene,[5] and nanodiamonds[6] exhibit outstanding electronic, optical, mechanical, and thermal properties.[7] Among them, NRBs are of special interest due to the tunable bandgap and high conductivity.[8–11] Especially, the properties of NRB are size-dependent, e.g., an NRB with more number of rings has less electron-phonon coupling, smaller band gap, and higher charge-carrier mobility.[12,13] While in acene family, tetracene is widely used for photoconductive material,[14] sensitizer[15] and molecular switches[16] because of the high carrier mobility of 0.01 cm^2/Vs on untreated SiO_2 insulator and 0.1 cm^2/Vs when chemically treated.[17–19]

Very recently, NRBs linked by four-membered rings are synthesized *via* a bottom-up method,[2] exhibiting an indirect band gap and ambipolar charge-transport character. Then an intriguing question arises: Can we further tune the band structure and change the band gap from indirect to direct? Here we answer this question by using fluorination and N-doping. In fact, fluorine has been widely used for modulating the properties of materials[20,21] because of the similar size, but different electronegativity, nitrogen doping in carbon-based materials become a popular strategy for effectively tuning the features of carbon.[22,23]

In this work, using density functional theory, we systematically study the properties of NRBs with three configurations, namely straight, zigzag and armchair, which exhibits an indirect band gap of 1.46, 0.73, and 0.32 eV, respectively. Moreover, the electronic band gap of these three configurations can be well tuned in the range of 0.0–1.47 by substituting hydrogen with fluorine atoms or changing from indirect to direct by doping with nitrogen, and the resulting structures are more stable than their hydrogenated analogs as confirmed by using AIMD simulations.

2. Computational Details

Calculations are based on density functional theory (DFT) as implemented in Vienna Ab initio Simulation package (VASP).[24,25] A vacuum space is introduced with a size of 13 Å for straight chain and 15 Å for zigzag and 9.33 Å for an armchair chain in a perpendicular direction to the chains for reducing the interactions with the periodic images. Lattice constants and atomic position both are optimized using a conjugate gradient method with energy and force criterion of 10^{-4} eV and 0.01 eVÅ^{-1} respectively. Projector augmented plan wave (PAW) method is used with a cutoff kinetic energy of 400 eV, and both Perdew-Burke-Ernzerhof (PBE)[26] and hybrid Hyed-Seuseria-Ernzerhof (HSE06)[27,28] are used for calculating electronic properties. Moreover, for investigating the thermal stability of all these configurations of tetracene nanoribbons, ab initio molecular dynamics (AIMD)[29] simulations are further performed with a time step of 1 fs.

3. Results and Discussion

3.1. Geometry and Stability

In the first step, we optimize the unit cells of all tetracene-based nanoribbons linked by four-membered rings. The unit cell with lattice constants of *(a* = 11.19 *b* = 9.74*)*, *(a* = 9.97 *b* = 14.48*)* and *(a* = 18.92 *b* = 11.30*)* for straight, zigzag and armchair configurations, respectively, as shown in Figure 1. In all configurations

[a] *U. Younis, I. Muhammad, Prof. Q. Sun*
Department of Material Science and Engineering
College of Engineering, Peking University
Beijing 10087, China
E-mail: sunqiang@pku.edu.cn
[b] *Prof. Y. Kawazoe*
New Industry Creation Hatchery Center
Tohoku University, Sendai, 980-8577, Japan
[c] *Prof. Y. Kawazoe*
Suranaree University of Technology
Nakhon Ratchasima 30000, Thailand
[d] *Prof. Q. Sun*
Center for Applied Physics and Technology
Peking University, Beijing 10087, China

Supporting information for this article is available on the WWW under https://doi.org/10.1002/cphc.201900803

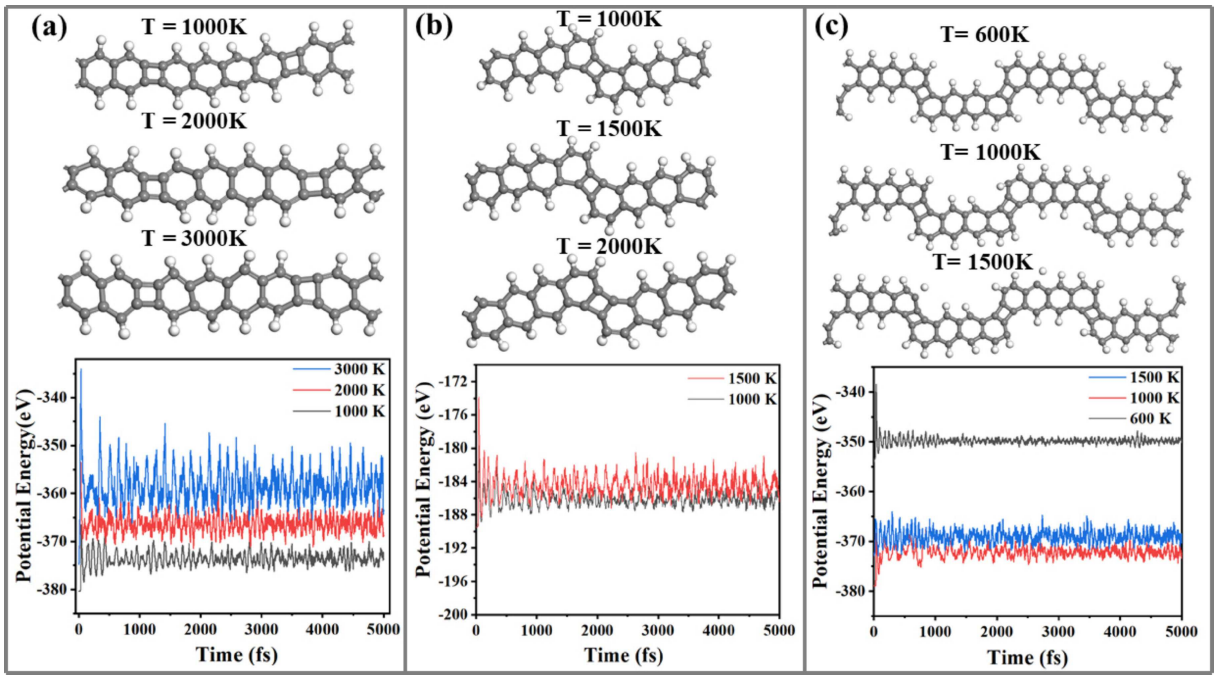

Figure 2. Potential energy fluctuations and snapshot configurations at different temperatures in MD simulations for a) straight, b) zigzag, and c) armchair TNRs.

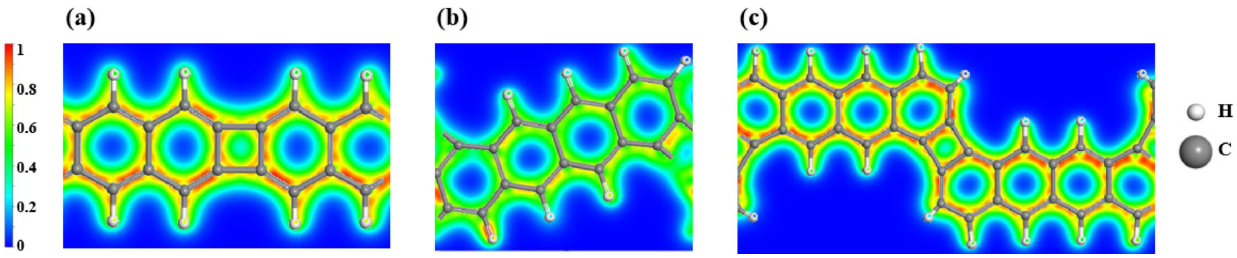

Figure 3. Electron localization function (ELF) of a) straight, b) zizag, and c) armchair TNRs.

of nanoribbons, hydrogen atoms, attached to the edge sites, are essential to maintain the structural stability. The bond length between C–C in all configurations of tetracene nanoribbons is 1.41 Å, while the C–H bond length is 1.09 Å. The C–C bond length in cyclobutadiene moieties of straight, zigzag and armchair chains are 1.48 Å, 1.52 Å and 1.49 Å respectively, the alteration in bond lengths modulates the electronic properties of a material.[30] The thermal stability of straight, zigzag and armchair chains are examined by using ab initio molecular dynamics (AIMD) simulations, within a 2×1×1 supercell at 1000, 2000 and 3000 K for 5 ps with a 1 fs time step. Figure 2 illustrates the fluctuation in potential energy for all configurations of TNRs at different temperatures. It can be seen that the straight chain is the most stable configuration which can maintain its structural stability at 3000 K, whereas the zigzag and armchair configurations can bear 2000 K and 1000 K respectively. This thermal stability analysis for TNR's shows that all the configurations are thermally stable and maintain their structure under high temperatures.

3.2. Electronic Properties

To better understand the bonding features, we calculate electron localization function (ELF) with values varying from 0 to 1, where zero corresponds to the completely delocalized electrons, and one to completely localized electron density, while 0.5 represents free electron behavior. The ELF results as plotted in Figure 3 display the covalent bonding features of C–C bond, which make TNRs semiconducting as shown in the band structures discussed below.[31]

We then calculate the density of states (DOS) and band structures, as shown in Figure 4. The PBE band gap for straight, zigzag and armchair nanoribbon is 0.94, 0.26, and 0.03 eV, respectively, while the corresponding value at HSE06 level is 1.46, 0.73, and 0.32 eV. Although the values are different, the indirect band gap is the characteristic feature for these configurations. Moreover, we calculate the band gap of all the configurations of tetracene nanoribbons under uniaxial-strain of 3% and 5%, and find that the band gaps of straight and

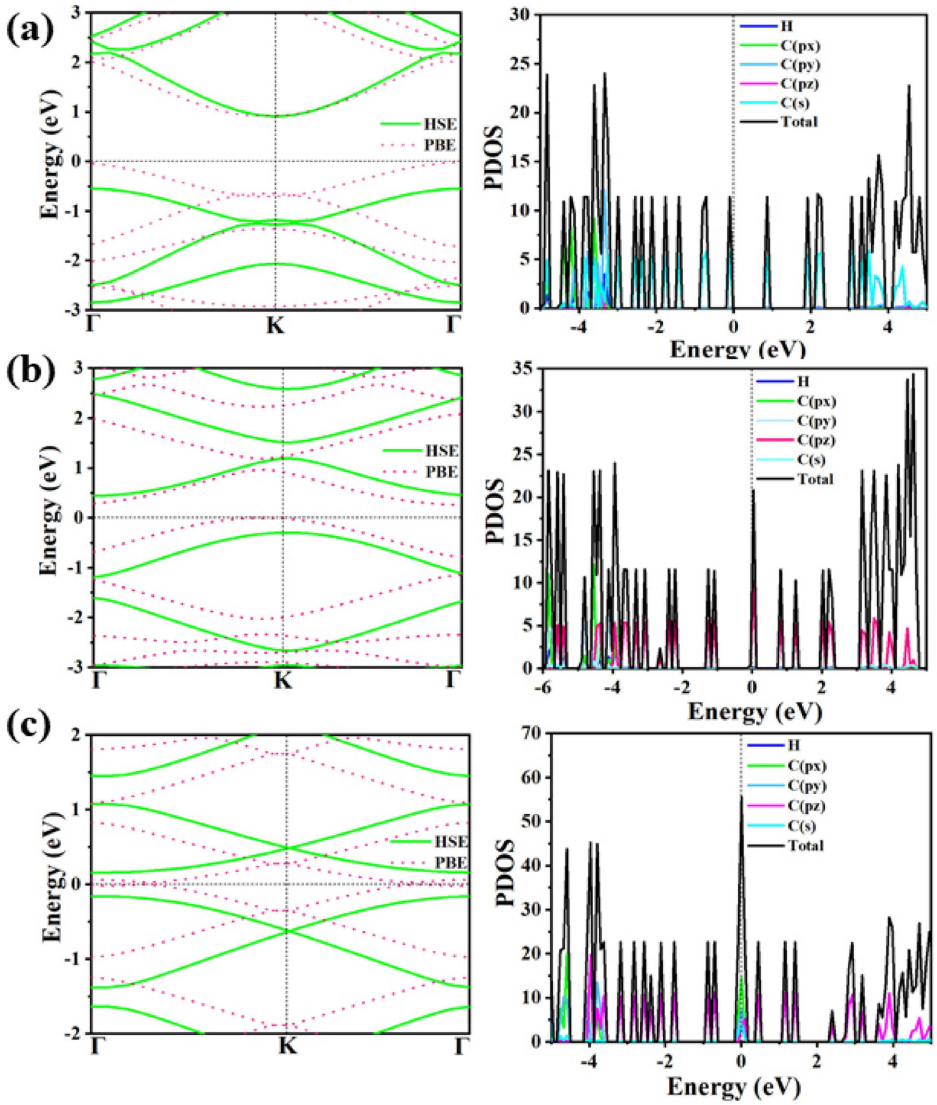

Figure 4. Band structure and partial density of states for a) straight, b) zigzag, and c) armchair TNRs using PBE and HSE06. The Fermi level is shifted to zero.

armchair TNRs are slightly increased while slightly decreased for zigzag TNR, and all the nanoribbons maintain their indirect nature of band gap. Therefore, strain is not effective in tuning the band gap of pristine TNRs. This motivates us to study F and N functionalized structures.

3.3. Band Tuning by Fluorine

Because of the similar size but different chemical properties of F as compared with that of H, fluorination has been widely used for functionalization of materials[32–34] In this study, fluorination is investigated in two different configurations: replacing half H in one side with F (labelled H–C–F) and replacing all H with F in two sides (labelled F–C–F) as shown in Figure 5. The band structures are calculated using both PBE and HSE06 functional as shown in Table 1 and Figure 6. One can see that the band gap of F-substituted system is reduced when increasing concentration of F-atoms. For half fluorinated structures of straight, zigzag and armchair TNR, band gap gets reduced to 1.40, 0.39 and 0.08 eV, which can be tuned to 1.32, 0.22, and 0.16 eV respectively when fully fluorinated. While for the

Table 1. Band gap tuning and charge transfer (CT) from the carbon atoms to the fluorine atoms using Bader charge analysis of pristine and F-substituted configurations of TNRs.

Configuration	Functional	Band gap tuning		
		H–C–H	H–C–F	F–C–F
straight	PBE	0.94 eV	0.87 eV	0.73 eV
	HSE06	1.46 eV	1.40 eV	1.32 eV
CT [e]			+0.62	+0.58
zigzag	PBE	0.26 eV	0 eV	0 eV
	HSE06	0.73 eV	0.39 eV	0.22 eV
CT [e]			+0.60	+0.60
armchair	PBE	0.03 eV	0.05 eV	0.07 eV
	HSE06	0.32 eV	0.08 eV	0.16 eV
CT [e]			+0.64	+0.63

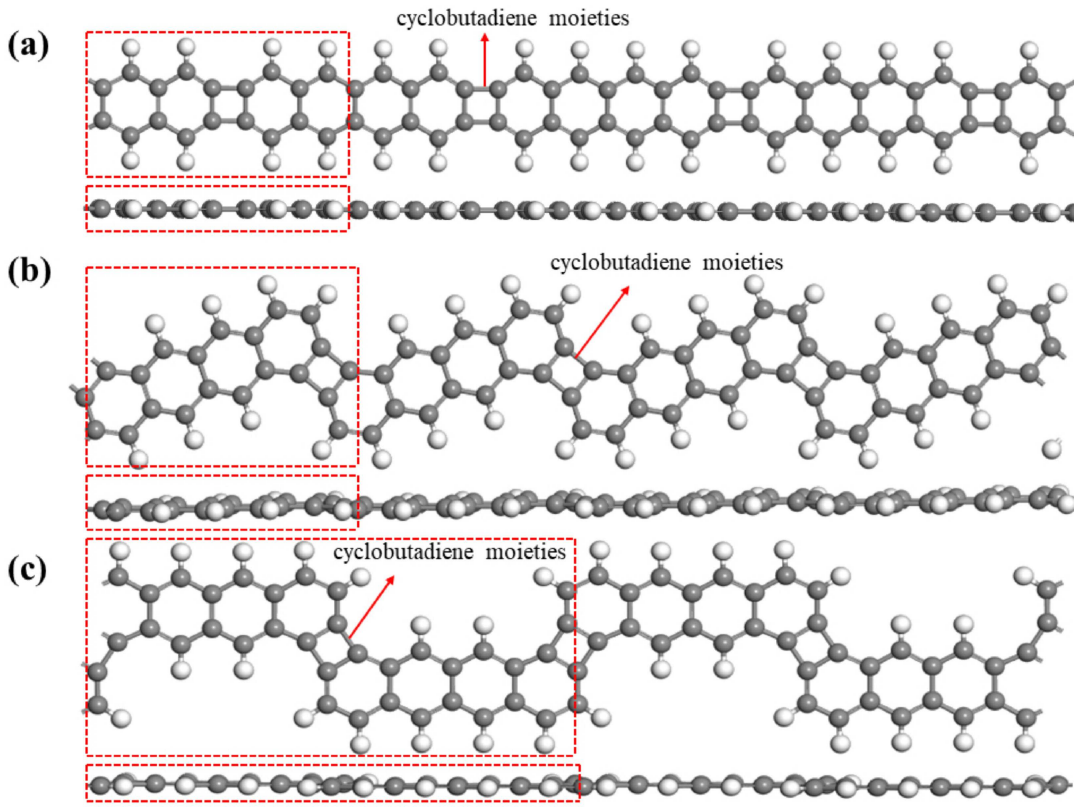

Figure 1. a) Straight, b) zigzag, and c) armchair configurations of tetracene nanoribbons incorporating four-membered rings. The unit cells are highlighted with dashed lines.

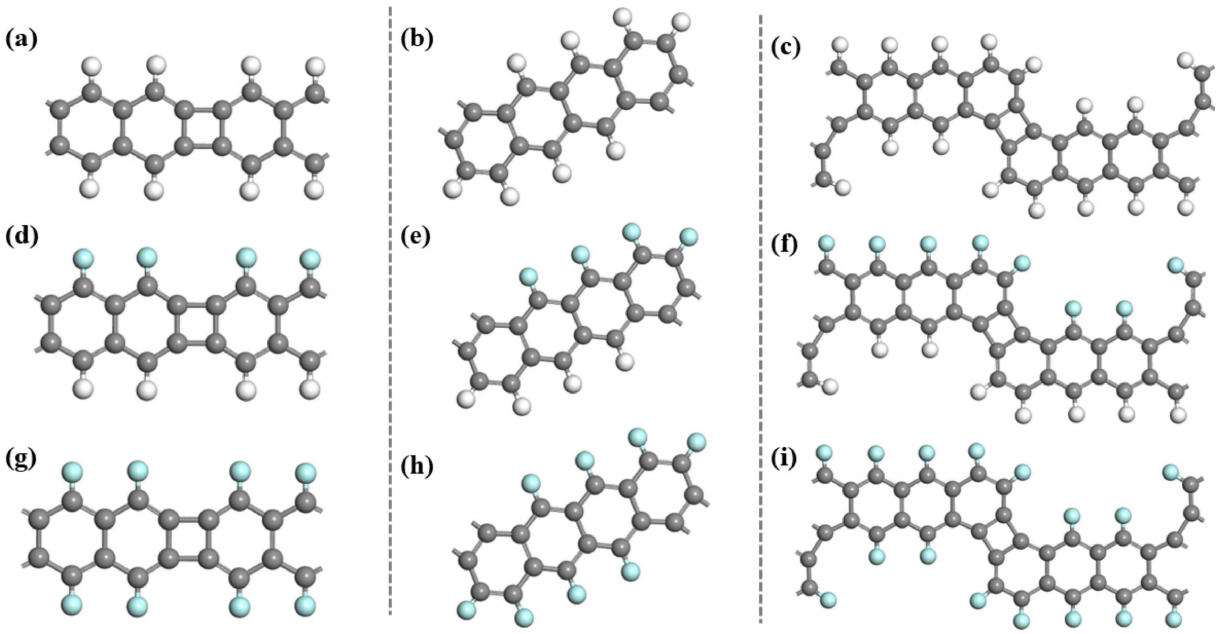

Figure 5. Geometric configuration of a)–c) pristine, d)–f) half, and g)–i) fully F-substituted TNRs.

armchair configuration, the band gap shows slight oscillations from half- to full-fluorination. The graphical variation of band gap by increasing the number of fluorine is given in Figure S1 in the Supporting Information (SI). Besides these three typical configurations, we have also studied other intermediate configurations by gradually substituting fluorine in straight, zigzag,

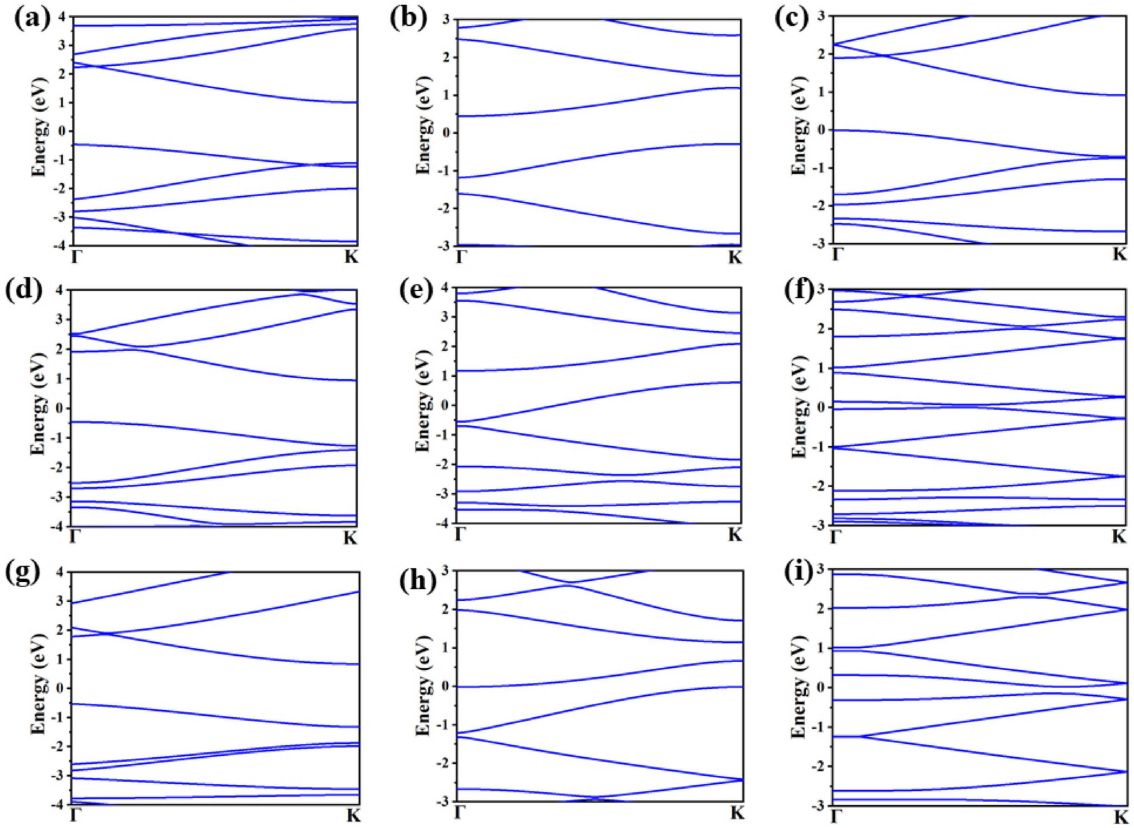

Figure 6. HSE06 band structure of (a–c) pristine, (d–f) half, and (g–i) fully F-substituted systems of straight (left panel), zigzag (middle panel), and armchair (right panel) configurations of TNRs.

and armchair, as shown in Figure S2, where the first fluorine is substituted at 1-para position in the first ring of the chain, in place of hydrogen, second fluorine is substituted at 4-para position in next ring, whereas third and fourth fluorines are substituted at alternate 1 and 4 para position in third and fourth ring respectively. One can see that the halogenation of 1D tetracene-based nanoribbons can efficiently tune the electronic properties, which may have vital applications in photonics and nano-electronics.[35]

We also calculate the charge transfer using Bader charge[36,37] analysis, as shown in Table. 1, showing that because of the high electronegative affinity of F, fluorine gains 0.58, 0.60 and 0.63 electrons in fully F-substituted straight, zigzag and armchair TNRs, respectively, the corresponding value is 0.64, 0.6 and 0.62 for the half-fluorinated cases.

3.4. Band Engineering Using Nitrogen Doping

Inspired by the previous studies on nitrogen doping in 1D and 2D carbon materials for modulating the electronic properties,[38–40] we investigate the effects of N-doping in TNRs on band gap. Figure 7 shows pristine, half, and fully nitrogen-doped configurations of TNRs. Although CH and N are isoelectric, their size and electronegativity are different. The band gap of N-doped configurations decreases slightly. More interestingly, unlike the feature of indirect band gap observed in pristine and fluorinated TNRs, N-doped configurations exhibit direct band gap nature as shown in Figure 8. The band gap is found to be 1.74, 0.70, and 0.65 eV respectively for half nitrogen-doped straight, zigzag and armchair TNRs; the corresponding values are 1.00, 0.42, and 0.46 eV for full N-doped cases. The band engineering from indirect gap to direct gap by N-doping provides an effective strategy of modulating properties for nanoelectronic and optoelectronic applications. The main results are summarized in Table 2, and the electron localization functions of all nitrogen-doped configurations are given in Figure S3, exhibiting the ionic bonding features between C and N due to the difference in electron affinities.

Table 2. Band gap (in eV) of straight, zigzag, and armchair configurations of TNRs by N-doping.

Configurations	Functional	Prisinte	Half doped	Fully doped
straight	PBE	0.94	1.18	0
	HSE06	1.46	1.74	1
zigzag	PBE	0.26	0.20	0
	HSE06	0.73	0.70	0.42
armchair	PBE	0.03	0.19	0
	HSE06	0.32	0.65	0.46

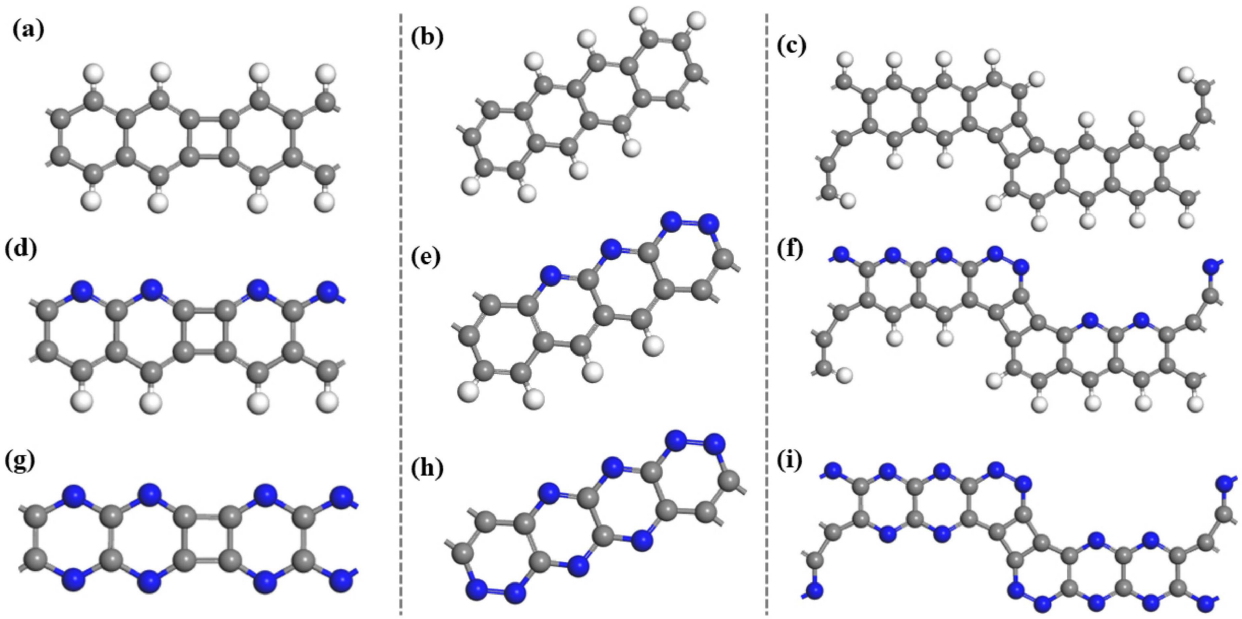

Figure 7. (a–c) Pristine, (d–f) half, and (g–i) fully N-doped configurations of straight (left panel), zigzag (middle panel), and armchair (right panel) TNRs.

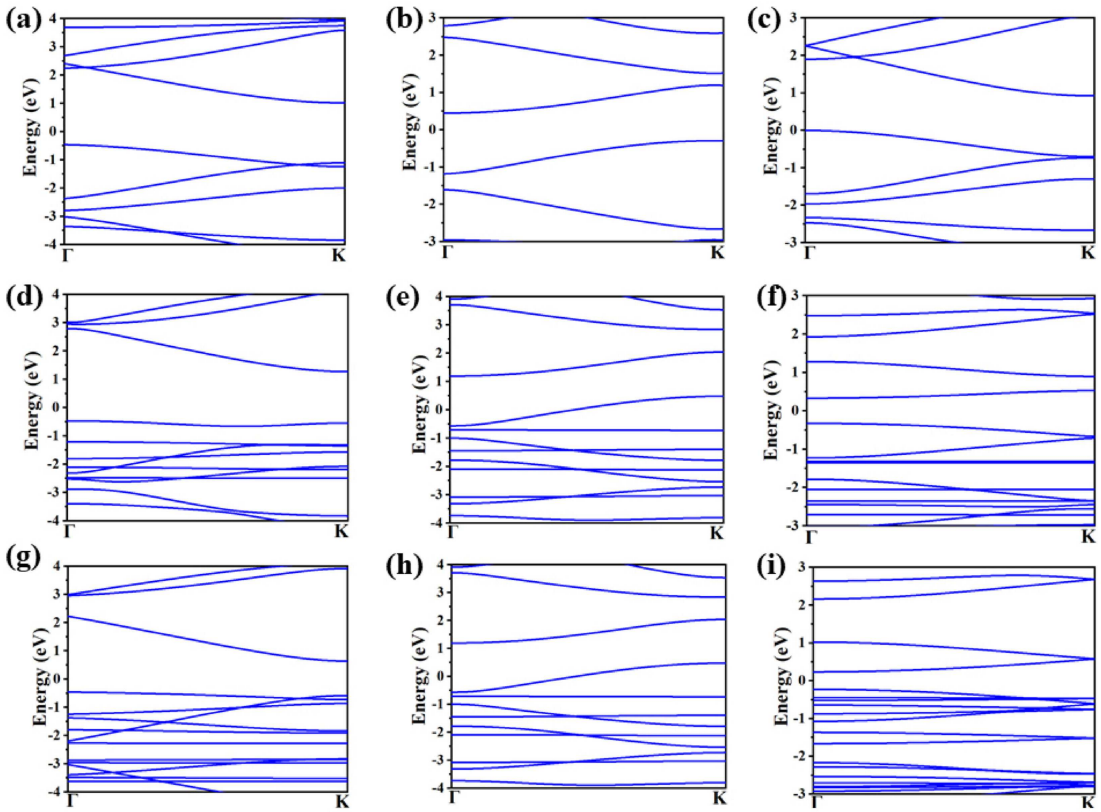

Figure 8. HSE06 band structure of (a–c) pristine, (d–f) half, and (g–i) full N-doped systems of straight (left panel), zigzag (middle panel), and armchair (right panel) configurations of TNRs.

4. Conclusions

Motivated by the recent experimental synthesis of tetracene-based nanoribbons, we performed density functional theory to study the thermal stabilities, electronic properties, and band engineering by replacing H with F or doping with N. Thermal stability analysis shows that the straight chain is most stable and can bear 3000 K without any structural breakage. The size of energy gap can be effectively tuned by introducing F-atoms with half and full fluorinations. For straight and zigzag configurations, the band gap decreases from C–H–H to H–C–F and F–C–F, while oscillations exist in an armchair configuration, suggesting that both ligand and geometry can modulate the band gap. Furthermore, nitrogen doping not only reduces the size of band gap but also can tune the nature of band gap from indirect to direct. The diversity of geometric configurations formed from tetracene unit together with the flexibility of band structure tuning suggests that tetracene based materials deserve more attention in future research.

Acknowledgements

This work is partially supported by grant from the National Natural Science Foundation of China (NSFC-21573008, -21773003), and from the Ministry of Science and Technology of China (2017YFA0204902). Y.K. is thankful to the support by AOARD for the grant of FA2386-18-1-4050. The calculations are supported by High-performance Computing Platform of Peking University.

Conflict of Interest

The authors declare no conflict of interest.

Keywords: doping · electronic properties · functionalization · stability · tetracene nanoribbons

[1] H. Sahin, O. Leenaerts, S. K. Singh, F. M. Peeters, *Wiley Interdiscip. Rev.: Comput. Mol. Sci.* **2015**, 1.
[2] C. Sánchez-Sánchez, C. Sánchez-Sánchez, T. Dienel, A. Nicolaï, N. Kharche, L. Liang, C. Daniels, V. Meunier, J. Liu, X. Feng, K. Müllen, J. R. Sánchez-Valencia, O. Gröning, P. Ruffieux, R. Fasel, *Chem.-A Eur. J.* **2019**.
[3] J. E. Anthony, *Chem. Rev.* **2006**, *106*, 5028.
[4] A. Mateo-Alonso, *Chem. Soc. Rev.* **2014**, *43*, 6311.
[5] T. Braun, A. P. Schubert, R. N. Kostoff, *Chem. Rev.* **2002**, *100*, 23.
[6] V. N. Mochalin, O. Shenderova, D. Ho, Y. Gogotsi, *Nat. Nanotechnol.* **2012**, *7*, 11.
[7] I. Muhammad, H. Xie, U. Younis, Y. Qie, W. Aftab, Q. Sun, *Nanoscale* **2019**, *11*, 9000.
[8] T. N. Rekha, B. J. M. Rajkumar, *Synth. Met.* **2016**, *215*, 207.
[9] L. E. de Sousa, A. A. Mamiya, J. Kjelstrup-Hansen, D. A. da Silva Filho, *J. Mol. Model.* **2017**, *23*.
[10] M. Watanabe, Y. J. Chang, S. W. Liu, T. H. Chao, K. Goto, M. M. Islam, C. H. Yuan, Y. T. Tao, T. Shinmyozu, T. J. Chow, *Nat. Chem.* **2012**, *4*, 574.
[11] Q. Chen, A. J. McDowall, N. V. Richardson, *Langmuir* **2003**, *19*, 10164.
[12] M. J. Panzer, C. D. Frisbie, *Appl. Phys. Lett.* **2006**, *88*, 1.
[13] J. E. Anthony, *Angew. Chem. Int. Ed.* **2008**, *47*, 452.
[14] T. Suzuki, T. Okamoto, A. Saeki, S. Seki, H. Sato, Y. Matsuo, *ACS Appl. Mater. Interfaces* **2013**, *5*, 1937.
[15] T. N. Rekha, B. J. M. Rajkumar, *Synth. Met.* **2016**, *215*, 207.
[16] P. Cui, Q. Zhang, H. Zhu, X. Li, W. Wang, Q. Li, C. Zeng, Z. Zhang, *Phys. Rev. Lett.* **2016**, *116*, 1.
[17] H. Moon, R. Zeis, E. J. Borkent, C. Besnard, A. J. Lovinger, T. Siegrist, C. Kloc, Z. Bao, *J. Am. Chem. Soc.* **2004**, *126*, 15322.
[18] B. Lu, H. J. Zhang, H. Huang, H. Y. Mao, Q. Chen, H. Y. Li, P. He, S. N. Bao, *Appl. Surf. Sci.* **2005**, *245*, 208.
[19] J. P. Calbert, D. A. S. Filho, J. Cornil, J. L. Bre, *Proc. Natl. Acad. Sci. USA* **2002**, *99*.
[20] J. Zhou, M. M. Wu, X. Zhou, Q. Sun, *Appl. Phys. Lett.* **2009**, *95*.
[21] J. Zhou, Q. Wang, Q. Sun, P. Jena, *Phys. Rev. B-Condens. Matter Mater. Phys.* **2010**, *81*, 1.
[22] K. R. Lee, K. U. Lee, J. W. Lee, B. T. Ahn, S. I. Woo, *Electrochem. Commun.* **2010**, *12*, 1052.
[23] Q. Shi, Y. Ma, L. Qin, B. Tang, W. Yang, Q. Liu, *ChemElectroChem* **2019**, *6*, 2924.
[24] F. Wende, M. Marsman, J. Kim, F. Vasilev, Z. Zhao, T. Steinke, *Int. J. Quantum Chem.* **2019**, *119*, 1.
[25] I. Muhammad, S. Wang, J. Liu, H. Xie, Q. Sun, *J. Renew. Sustain. Energy* **2019**, *11*, 014106.
[26] E. W. Smeets, J. Voss, G. J. Kroes, *J. Phys. Chem. A* **2019**.
[27] J. Heyd, G. E. Scuseria, M. Ernzerhof, *J. Chem. Phys.* **2003**, 118, 8207.
[28] P. G. Moses, M. Miao, Q. Yan, C. G. Van De Walle, *J. Chem. Phys.* **2011**, 134, 084703.
[29] M. A. Blanco, H. W. Hatch, J. E. Curtis, V. K. Shen, *J. Chem. Phys.* **2018**, 149, 084203.
[30] N. N. Karaush, G. V Baryshnikov, B. F. Minaev, *Chem. Phys. Lett.* **2014**, *612*, 229.
[31] V. Georgakilas, M. Otyepka, A. B. Bourlinos, V. Chandra, N. Kim, K. C. Kemp, P. Hobza, R. Zboril, K. S. Kim, *Chem. Rev.* **2012**, *112*, 6156.
[32] B. Bhattacharya, N. B. Singh, U. Sarkar, *J. Phys. Conf. Ser.* **2014**, *566*.
[33] R. Ponce Ortiz, R. Malavé Osuna, M. C. Ruiz Delgado, J. Casado, V. Hernández, J. T. López Navarrete, Y. Sakamoto, T. Suzuki, *Org. Optoelectron. Photonics II* **2006**, *6192*.
[34] D. Wu, S. Wang, J. Yuan, B. Yang, H. Chen, *Phys. Chem. Chem. Phys.* **2017**, *19*, 11771.
[35] N. Wei, Y. Chen, K. Cai, J. Zhao, H. Q. Wang, J. C. Zheng, *Phys. Chem. Chem. Phys.* **2016**, 1.
[36] G. Henkelman, A. Arnaldsson, H. Jonsson, *Comput. Mater. Sci.* **2006**, *36*, 354.
[37] M. Yu, D. R. Trinkle, *J. Chem. Phys.* **2011**, 134, 064111.
[38] L. Chen, L. Wang, Z. Shuai, D. Beljonne, *J. Phys. Chem. Lett.* **2013**, *4*, 2158.
[39] M. Makaremi, S. Grixti, K. T. Butler, G. A. Ozin, C. V. Singh, *ACS Appl. Mater. Interfaces* **2018**, *10*, 11143.
[40] Z. Liu, J. S. A. Ishibashi, C. Darrigan, A. Dargelos, A. Chrostowska, B. Li, M. Vasiliu, D. A. Dixon, S. Y. Liu, *J. Am. Chem. Soc.* **2017**, *139*, 6082.

Manuscript received: August 10, 2019
Revised manuscript received: August 22, 2019
Accepted manuscript online: August 24, 2019
Version of record online: ■■, ■■■

ARTICLES

Tune the gap! The band gaps of tetracene-based nanoribbons can be effectively tuned by substituting hydrogen with fluorine atoms and by doping with nitrogen atoms. This is shown for different configurations, namely straight, zigzag, and armchair nanoribbons.